RSC Pharmaceutics

Accepted Manuscript

This article can be cited before page numbers have been issued, to do this please use: B. Valamla, P. S. Chary, U. Anuradha, K. K. Parida, N. P. Kalia and N. K. Mehra, *RSC Pharm.*, 2026, DOI: 10.1039/D5PM00345H.

Development and Evaluation of Fenticonazole Nitrate Loaded Fucoidan Crafted Lecithin Chitosan Nanoparticles for the Treatment of Vaginitis

Valamla Bhavana[1], Padakanti Sandeep Chary[1], Urati Anuradha[2], Kishan Kumar Parida[2], Nitin Pal Kalia[2], Neelesh Kumar Mehra[1] *

[1]Pharmaceutical Nanotechnology Research Laboratory, Department of Pharmaceutics, National Institute of Pharmaceutical Education and Research (NIPER), Hyderabad, Telangana, INDIA 500037

[2]Department of Biological Sciences, National Institute of Pharmaceutical Education and Research (NIPER), Hyderabad, Telangana, INDIA 500037

Corresponding Author

Neelesh Kumar Mehra, PhD

Pharmaceutical Nanotechnology Research Laboratory,

Department of Pharmaceutics

National Institute of Pharmaceutical Education and Research (NIPER)

Ministry of Chemicals and Fertilizers, Government of India, Hyderabad,

Telangana, INDIA 500 037

Tel: +91-8839030437, +91-40-230747750

E-mail: neelesh@niperhyd.ac.in; neelesh81mph@gmail.com

View Article Online
DOI: 10.1039/D5PM00345H

Abstract

In this investigation, self-assembling nanoparticles Fenticonazole loaded lecithin chitosan nanoparticles (FZNP) with cationic zeta potential was altered by coating them with anionic fucoidan polymer (Fu-FZNP) through ionic gelation method to overcome vaginal mucosal barrier. The particle size of FZNP and Fu-FZNP were 129.20±0.25 nm and 227.10±1.54 nm, polydispersity index was 0.21±0.00, 0.26±0.01 and zeta potential were 30.96±1.15 mV and -26.75±0.3. The entrapment efficiency and drug loading were 65.47± 2.32% and 11.69±0.414% for FZNP, 71.13±5.74% and 7.41±0.60% for Fu-FZNP, respectively. The nanoparticle exhibited spherical and smooth morphology under TEM imaging. An excised goat vagina was used for the *ex-vivo* permeation studies, drug permeation was observed 61.74±2.07% for FZNP and 72.11±1.4% for Fu-FZNP. FZNP and Fu-FZNP demonstrated antibacterial and antifungal properties against *Staphylococcus aureus* and *Candida albicans*, respectively, *in-vitro*. Therefore, FZN and Fu-FZNP lecithin chitosan nanoparticles may be developed further for the safe, practical, and efficient treatment of mixed vaginal infections.

Keywords: Lecithin chitosan nanoparticles, fucoidan, zeta potential altering nanoparticles

View Article Online
DOI: 10.1039/D5PM00345H

1. Introduction

Vaginal infection is a chronic gynecological issue in women of reproductive age that can lead to various health complications. Mixed vaginitis, which occurs rarely is caused by the presence of two vaginal pathogens (bacterium and candida species), necessitating the usage of dual therapy with a combination of antifungal and antibacterial drugs or broad-spectrum monotherapy to eliminate concurrent symptoms[1][2][3] .

Fenticonazole is an imidazole derivative with antifungal properties that was created about thirty years ago to treat dermatomycosis and candida vaginitis topically. **Fenticonazole nitrate** (FZN) has demonstrated extensive antimycotic action against yeasts and dermatophytes in both *in-vitro* and clinical investigations[4], [5]. Three distinct mechanisms that allow fenticonazole to perform its specific antimycotic activity action: (i) reduction of *candida albicans* protease acid secretion, (ii) cytoplasmic membrane damage, and (iii) blockage of cytochrome oxidase and peroxidases [6][3], [7], [8], [9]. Fenticonazole nitrate is commercially available in conventional dosage forms such as vaginal creams, ovules, and pessaries (e.g., 2% vaginal cream and 600 mg vaginal ovules), which are commonly prescribed for vulvovaginal candidiasis and mixed infections. However, these formulations suffer from limitations such as poor retention at the vaginal site, frequent dosing, and reduced patient compliance.

Two additional pharmacological properties of Fenticonazole are noteworthy. The drug persists in the skin's stratum corneum for a prolonged period. It has unique pharmacokinetic properties that enable the accumulation of the active drug in mucosal tissue for up to 72 h. This accumulation forms a reservoir of FZN, delaying the need for consecutive administrations. Moreover, the assessment of Fenticonazole plasma levels has validated the drug's inadequate systemic absorption. Consequently, for mixed infections comprising mycotic, bacterial, dermatophyte, and/or *Trichomonas* species, Fenticonazole may be the perfect topical substitute for combination therapy[10], [11], [12].

Vaginal route is an essential mode of drug delivery to treat local and systemic ailments. The vaginal route has a few benefits due to its large surface area, adequate blood supply, lack of first-pass effect, slightly greater drug permeability, and self-insertion simplicity[13]. The literature suggests using inventions that attach to vaginal mucosa *via* forming chemical and physical bonds with the mucus as one way to solve the issue. Mucosal drug delivery is intrinsically challenging since vaginal medication distribution is constrained by presence of anatomical and physiological factors[14], [15], [16].

View Article Online
DOI: 10.1039/D5PM00345H

Many medical conditions, such as cancer, fungus, and bacterial infections, can be treated and prevented with the use of vaginal drug delivery[17]. The high porosity, negative charge, high porosity and interconnectivity, hydrophilic and hydrophobic regions of the vaginal microenvironment contribute to the barrier properties of vaginal drug delivery. In order to enhance the vaginal delivery of active substances, mucoadhesive and mucus-penetrating particles were designed by adjusting their chemical constituents, surface characteristics, size, and amount of surface functionalization[18], [19].

The advancement of nanotechnology in recent times has created novel pathways i.e, using muco-adhesive polymers, mucus penetrating polymers and zeta potential modifying polymers to overcome the vaginal mucosal barriers[20] [21] [22]. A naturally occurring polycationic polymer, chitosan is created when chitin undergoes partial deacetylation. Chitosan has the added benefit of being naturally derived, which makes it biodegradable, biocompatible with good bioadhesive properties[23]. Chitosan is being utilized to produce nanoparticles via ionotropic gelation with tripolyphosphate[24], [25]. Furthermore, this has been studied for the stabilization of microemulsion with lecithin combination as emulsifying agent[26]. Lecithin is a phospholipid combination that is commonly utilized to make liposomes and micelles[27], [28]. Interestingly, encapsulating these lipid-based nanostructures with chitosan has been shown to improve their stability and give mucoadhesive properties[29], [30], [31]. In recent years, films and gels build around the bonding between negatively charged phospholipids and chitosan have been considered for the transport of lipophilic drugs[32], [33]. Fucoidan is a sulfated polysaccharide with a high density of negatively charged sulfate groups, which plays a crucial role in modulating the surface charge (zeta potential) of lecithin–chitosan nanoparticles. This modulation reduces excessive mucoadhesion while promoting mucus penetration by minimizing electrostatic interactions with negatively charged mucins. Additionally, fucoidan's bioactive properties, including anti-inflammatory and antimicrobial effects, further enhance its suitability for vaginal drug delivery.

The lecithin-chitosan nanoparticles are the promising drug carriers formed by the supramolecular self- organizing electrostatic interactions between negatively charged lecithin and positively charged chitosan[34], [35], [36]. Melatonin, quercetin, and diflucortolone valerate loaded chitosan/lecithin nanoparticles are just a few examples in this study[37][38][39][40].

Mucus gets digested, excreted, regenerated, and secreted continually. Mucus has a brief turnover time, frequently measured in minutes to hours, especially for the poorly adhering mucus layer. Effective particle clearance is achieved by the vaginal mucus output rate of about

View Article Online
DOI: 10.1039/D5PM00345H

6 mL/day for vaginal medication delivery. Therefore, there is need to develop smart delivery schemes which initially don't interact with mucus and later adhere to the membrane and mucus to overcome the continuedly cleared mucus[41], [42], [43]. To circumvent the drawbacks of available vaginal drug delivery while preserving and even refining security profiles, a novel vaginal drug delivery was developed by surface modification of positively charged lecithin chitosan nanoparticles with negatively charged fucoidan to alter the zeta potential of the system.

2. Materials and Methods

2.1 Materials

The Fenticonazole was arranged as gift sample from optimus Pharma, Hyderabad. Fucoidan, Chitosan was purchased from the Sigma-Aldrich, St. Louis, Missouri, USA. The essential oils (lemongrass oil, lavender oil) were procured from the Botanical Healthcare (Bangalore, India). The solvents like methanol were brought form SRL Chemicals, India of HPLC analytical grade. The polyvinyl alcohol (98-99% hydrolysis) was procured from Loba Chemie (Mumbai, India) and hyaluronic acid from PC CHEM, Mumbai, India. The deionized water was used for the studies and the other chemicals were used as such received from the distributors.

2.2 Methodology

2.2.1 Preparation of Fenticonazole nitrate lecithin chitosan nanoparticles (FZNP)

The novel antifungal formulation development involves preparation of self-assembling nanoparticles as shown in **Figure 1**. The ethanol injection method based on ionic interaction technique was exploited to prepare lecithin chitosan nanoparticles. Initially, 0.2% chitosan (w/v) aqueous phase solution in 1% glacial acetic acid was placed on magnetic stirrer (Remi, Mumbai) for 16 h (solution A). For nanoparticles preparation, FZN was solubilized in ethanolic solution containing lecithin (solution B). In short, the formulation was acquired by swiftly injecting solution B from syringe into solution A that was stirred uninterruptedly at 500±10 rpm on the magnetic stirrer. The various batches of the nanoparticles were formulated to develop stable formulation as illustrated in **Table 1**.

View Article Online
DOI: 10.1039/D5PM00345H

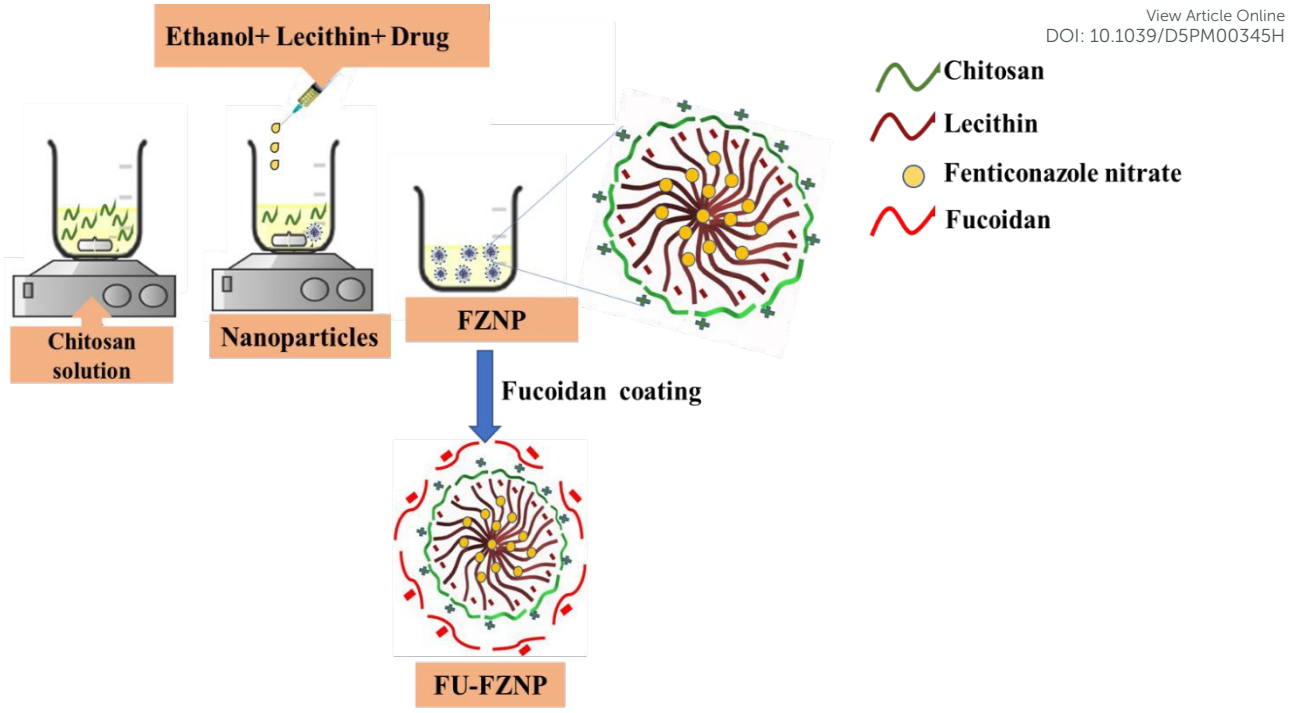

Figure 1: Schematic representation of Fenticonazole nitrate loaded fucoidan lecithin chitosan nanoparticles by ethanol injection method.

2.2.2 Preparation of Fenticonazole nitrate loaded fucoidan coated lecithin chitosan nanoparticles (Fu-FZNP)

The above prepared nanoparticles with positive zeta potential were further coated with negatively charged fucoidan (Fu) to obtain zeta potential altering nanoparticles to overcome the interaction with negatively charged mucus barrier as shown in Figure 1. Surface coating of nanoparticles with fucoidan was carried out by a post-fabrication adsorption method. Fucoidan was dissolved in deionozed water. An accurately measured volume of the nanoparticle suspension was added dropwise to the fucoidan solution to achieve a nanoparticle-to-fucoidan stoichiometric ratio (1:2 w/w). The mixture was incubated under gentle stirring at room temperature for 2 h to allow electrostatic interaction and adsorption of fucoidan onto the nanoparticle surface.

Fucoidan and chitosan are multifunctional polymers which are capable of being ionized in an aqueous medium. Fucoidan can be expressed as FU−COOH−SO_3H/FU−COO−−SO_3^- , and chitosan as CHI-NH_3^+/ CHI-NH_2 in their protonation and deprotonation forms. The ionic cross linking relies on the chitosan and fucoidan favorable electrostatic contact, the quantity of ionizable locations on the surface of the polymers will determine its outcome. Table 1 illustrates how fucoidan was added to the previously optimized batch. Particle size and zeta potential of the resultant nanoparticles were further examined. Rhodamine B was incorporated

View Article Online
DOI: 10.1039/D5PM00345H

into the nanoparticles for ***ex-vivo*** permeation studies by replacing fenticonazole nitrate with rhodamine B during the nanoparticle preparation process, following the same formulation protocol. The dye was dissolved in the aqueous phase prior to nanoparticle formation, allowing its entrapment within the nanoparticulate matrix. The nanoparticles were freeze dried for further analysis.

2.2.3 Physicochemical characterization of lecithin chitosan nanoparticles

2.2.3.1 Particle size, PDI and zeta potential

Particle size, PDI and zeta potential of FZNP and Fu-FZNP were examined by Zeta sizer (NanoZ S Malvern, UK). The polystyrene cuvettes were occupied with nanoparticles solutions and analyzed at 173° scattering angle and 25 ± 0.5°C temperature. All the samples were examined in triplicates and reported as mean±SD (n=3)[44][45].

2.2.3.2 ATR -FTIR analysis of nanoparticles

The spectroscopic analysis of chitosan (CH), fucoidan (Fu), FZN, PM (physical mixture of lecithin, chitosan, fucoidan, drug in 1:1:1 ratio), freeze-dried blank chitosan lecithin nanoparticles (BNP), FZNP and Fu-FZNP were examined using ATR -FTIR (spectrum RX-1 Perkin Elmer, US). Separately, 5mg of freeze-dried samples were placed on the holder and scanned at a resolution of 4 covering a wavenumber spectrum of 400 –4000 cm $^{-1}$[46] [47].

2.2.3.3 Differential scanning calorimetry (DSC) analysis of nanoparticles

DSC was used to measure the thermodynamic events of excipients and drug (STARe system, Metler Toledo, Switzerland). After weighing the samples (chitosan, fucoidan, FZN, PM, BNP, FZNP and Fu-FZNP), they were positioned in an aluminium pan and heated to an elevated temperature in compliance with the protocol while flowing 50mL/min of liquid nitrogen through it. The samples were analysed at temperature ranging from 25 to 300° for 10 minutes[48].

2.2.3.4 P-XRD analysis of nanoparticles

The PXRD (Empyrean, Malvern Panalytical, Worcestershire, United Kingdom) of chitosan, fucoidan, FZN, PM, BNP, FZNP and Fu-FZNP were performed. The freeze-dried samples were examined at a speed of 0.0436°/sec and at angles ranging from 2 to 40° (2Θ)[49], [50].

2.2.3.5 Surface morphology by Transmission electron microscopy (TEM)

The morphology and structure of FZNP and Fu-FZNP were evaluated with the help of TEM (JEM1400 TEM; JEOL, Tokyo, Japan) with 500 K magnification and 120 Kv illumination installed at the National Institute of Animal Biology (NIAB), Hyderabad. The nanoparticles

View Article Online
DOI: 10.1039/D5PM00345H

were allowed to dry on a small carbon-coated grid and viewed with microscope at a proper magnification. The samples were prepared on a carbon grid and negative stained with a 1% uranyl acetate. Microphotographs of FZNP and Fu-FZNP were clicked at appropriate magnification[51].

2.2.4 Drug loading and Entrapment efficiency

The entrapment efficiency and drug loading of FZNP and Fu-FZNP were estimated by indirect technique with the aid of RP- HPLC at 252 nm wavelength. The FZNP and Fu-FZNP were centrifuged (Micro ultracentrifuge, sorval Mx150+, Thermo Fisher Scientific, US) at 50,000±100 rpm for 2 h at 4±0. 5°C. Following centrifugation, the clear supernatant containing the unentrapped drug was carefully collected without disturbing the nanoparticle pellet. To ensure complete removal of surface-associated drug, the nanoparticle pellet was washed twice with buffer, followed by centrifugation under the same conditions. The wash supernatants were pooled with the initial supernatant. The supernatant was collected, and methanol was used as diluent and further analyzed by RP- HPLC, based on a previously constructed calibration curve. The % entrapment efficiency and drug loading were estimated by equations 3.1 and 3.2.

$$\%\ \text{Entrapment efficiency} = \frac{\text{Drug entrapped in pellet}}{\text{Amount of drug added}} \times 100 \quad \ldots\ldots \text{Equation 2.1}$$

$$\%\ \text{Drug loading} = \frac{\text{Entrapped drug amount}}{\text{Amount of lipid used}} \times 100 \quad \ldots\ldots\ldots\ldots\ldots\ldots \text{Equation 2.2}$$

2.2.5 *In-vitro* interaction of mucin with FZNP and Fu-FZNP

To study the *in-vitro* interaction of mucin with the developed nanoparticles gastric mucin was used. A 1mL mucin solution (2 mg/mL) was combined with 1 mL of FZNP and Fu-FZNP and the mixture was constantly agitated for 1 h at 37±0.5ºC[52]. The particle size and zeta potential of the nanoparticles were measured using a zeta sizer. All measurements were performed in triplicates and noted as an average with standard deviation.

2.2.6 *Ex-vivo* permeation studies

Fresh goat vaginal mucosa was obtained from a local abattoir from healthy adult animals of approximately [6–12 months] immediately after slaughter. The excised tissue was washed with cold normal saline to remove adhering blood and debris and transported to the laboratory in ice-cold phosphate-buffered saline (PBS, pH 7.4) within 1–2 h of collection. Upon arrival, excess connective tissue and fat were carefully removed, and the mucosal layer was separated using blunt dissection. The tissue was stored at 4 °C in PBS and used within 24 h to preserve

View Article Online
DOI: 10.1039/D5PM00345H

viability. Fresh goat vaginal mucosa procured from the slaughterhouse was placed below the donor compartment and above the receptor compartments of a locally constructed Franz's diffusion cell, which had a diffusion area of 4.9 cm^2, to test *ex-vivo* permeation. The FZNP and Fu-FZNP samples were positioned into the cell donor. The receptor compartment was kept at 37±0.5ºC and contained 25 mL of simulated vaginal fluid (pH 4.5) with 25% methanol to create a sink condition. Parafilm was used to properly seal the system. A suitable number of fresh media was added to replace the 0.5 mL that had been removed. The collected samples were passed through 0.45 µm membrane filter and analyzed by validated HPLC method at a wavelength of 252 nm. The permeation flux ($J_{max)}$ was assessed by the consecutive equation 3.3[53]:

$$J_{max}=\frac{\text{Amount of FZN Permeated}}{\text{Time} \times \text{Area of membrane}} \quad \text{Equation 2.3}$$

2.2.7 *In-vitro* antimicrobial activity

The *Staphylococcus aureus (S. Aureus)* (ATCC 29213) and *Candida albicans (C. albicans) (MTCC 183)*, Gram-positive bacterial and fungal strain, were exploited to estimate the antimicrobial activity of FZN, FZNP and Fu-FZNP. The stock cultures were kept at 4°C on sabouraud dextrose agar medium for fungi and Muller-Hinton Agar for bacteria. The antibacterial activity was investigated using the agar-well diffusion method. The tests were run on sabouraud dextrose agar for fungus and Muller-Hinton Agar for bacteria. For 24 h at 30°C for bacteria and 48 h at 37°C for fungi, the samples were placed on the plates and incubated. A zone of inhibition representing the antibacterial and antifungal activity was identified. Photos and a report on the inhibition zone's diameter were taken.

2.2.8 Stability study of FZNP and Fu-FZNP

The stability studies of the samples were performed 5±3ºC and 25±3ºC for 1 month. The samples were tested for physical appearance, particle size, PDI, zeta potential and entrapment efficiency. All the samples were analyzed in triplicates and reports as mean±SD.

2.2.9 Statistical Analysis

The experimental data are presented as mean ± standard deviation (SD). Statistical analysis was performed using analysis of variance (ANOVA) or Tukey's multiple comparison test in GraphPad Prism version 8.0 (GraphPad Software Inc., CA, USA). A p-value of less than 0.05 was considered statistically significant.

View Article Online
DOI: 10.1039/D5PM00345H

3. Results and Discussion

3.1 Optimization of FZNP and Fu-FZNP

A total of thirty-six batches were designed, developed, and characterized by varying process and excipients related attributes. The batches were optimized based on physical appearance, particle size, PDI and zeta potential as shown in Table 1. In the current work, ethanolic lecithin/FZN solution was injected into an aqueous chitosan solution to successfully produce lecithin chitosan nanoparticles. As illustrated in Figure 1, positively charged chitosan and negatively charged lecithin interacted through self-assembly. The resulting nanoparticles were found clear and blue in appearance. As indicated in Table 1, their characteristics were determined by measuring the mean particle size, zeta potential and PDI. It is believed that the positively charged chitosan covering the nanoparticles surface is the cause of their higher positive zeta potential.

The material attributes utilized in the optimization of the formulation were concentration of drug, lecithin, chitosan, fucoidan followed by process parameters including stirring speed and rate of addition. The amount of lecithin, chitosan and fucoidan had positive effect on size and PDI. The stirring speed and rate of addition had negative effect on size. The concentration of lecithin was fixed to 25 mg and chitosan to 3 mg and drug varied from 5 mg to 10 mg as the optimized batch with stirring speed 500 rpm. The zeta potential was increased with increase in chitosan amount and decreased with increase in lecithin amount. The fucoidan addition for altering the zeta potential resulted in increased particle size and negative potential of Fu-FZNP. The optimized batch was further characterized and evaluated.

Table 1: Pharmaceutical composition and optimization of the lecithin chitosan nanoparticles fabrication.

Batches	Lecithin (mg)	Chitosan (mg)	Fucoidan (mg/ml)	Stirring speed (rpm)	FZN (mg)	Size (nm)	PDI	Zeta potential (mV)
FZNP-1	37.5	3	0	400	10	140.7	0.22	+37.57
FZNP-2	50	3	0	300	5	125.3	0.24	+34.78
FZNP-3	50	2.25	0	400	10	202.3	0.28	+37.12
FZNP-4	25	3	0	400	5	129.2	0.20	+34.78
FZNP-5	50	1.5	0	200	10	169.7	0.27	+37.03
FZNP-6	25	2.25	0	200	5	117.5	0.20	+36.67
FZNP-7	25	1.5	0	300	10	135.8	0.24	+31.42
FZNP-8	37.5	2.25	0	300	7.5	146.0	0.26	+25.70

FZNP-9	50	3	0	200	7.5	156.3	0.25	+41.19
FZNP-10	50	1.5	0	400	5	215.5	0.22	+10.35
FZNP-11	25	3	0	200	10	179.3	0.23	+41.27
FZNP-12	25	1.5	0	400	7.5	221.4	0.38	+45.10
FZNP-13	25	1.5	0	500	5	186.2	0.23	+45.46
FZNP-14	50	1.5	0	500	10	230.4	0.34	+61.88
FZNP-15	50	3	0	300	5	264.2	0.37	+56.19
FZNP-16	25	1.5	0	300	5	297.3	0.28	+41.98
FZNP-17	50	1.5	0	300	10	271.8	0.33	+55.14
FZNP-18	25	3	0	500	10	178.7	0.20	+58.73
FZNP-19	50	3	0	500	5	325.9	0.38	+53.22
Fu-FZNP-1	25	1.5	1.5	500	5	288.2	0.28	-38.20
Fu-FZNP-2	50	1.5	1	500	10	302.0	0.30	-49.91
Fu-FZNP-3	50	3	1	300	5	387.8	0.36	-37.61
Fu-FZNP-4	25	1.5	1	300	5	313.3	0.30	-37.79
Fu-FZNP-5	50	1.5	1.5	300	10	299.8	0.34	-46.07
Fu-FZNP-6	25	3	1	500	10	210.0	0.21	-21.32
Fu-FZNP-7	25	3	1.5	300	10	254.4	0.27	-45.19
Fu-FZNP-8	50	3	1.5	500	5	331.4	0.34	-46.55
Fu-FZNP-9	37.5	3	1	400	10	216.4	0.20	-34.63
Fu-FZNP-10	25	3	0.5	400	5	220.2	0.15	-16.16
Fu-FZNP-11	50	1.5	0.5	200	10	241.9	0.23	-19.18
Fu-FZNP-12	25	2.25	1	200	5	227.1	0.26	-26.75
Fu-FZNP-13	25	1.5	1	300	10	197.8	0.22	-36.65
Fu-FZNP-14	37.5	2.25	0.5	300	7.5	238.7	0.43	-19.11
Fu-FZNP-15	50	3	1	200	7.5	191.0	0.15	-40.89
Fu-FZNP-16	50	1.5	1	400	5	260.6	0.22	-29.75

3.2 Physicochemical Characterization of Nanoparticles

3.2.1 Particle size, PDI and zeta potential of nanoparticles

The dynamic light scattering method was utilized to analysis the particle size and PDI. The particle size of optimized formulations FZNP and Fu-FZNP were found to be 129.20±0.25 nm and 227.10±1.54 nm, and the PDI was found to be 0.21±0.003 and 0.26±0.01 as shown in

View Article Online
DOI: 10.1039/D5PM00345H

Figure 2IC and 2IIC. The zeta potential of FZNP and Fu-FZNP were found to be +30.96±1.5 mV and -26.75±0.3 mV respectively as shown in Figure 2ID and 2IID. The particle size of the nanoparticles is increased upon coating of fucoidan, and the zeta potential changed from positive in FZNP to negative in Fu-FZNP indicating the formation of modified nanoparticles.

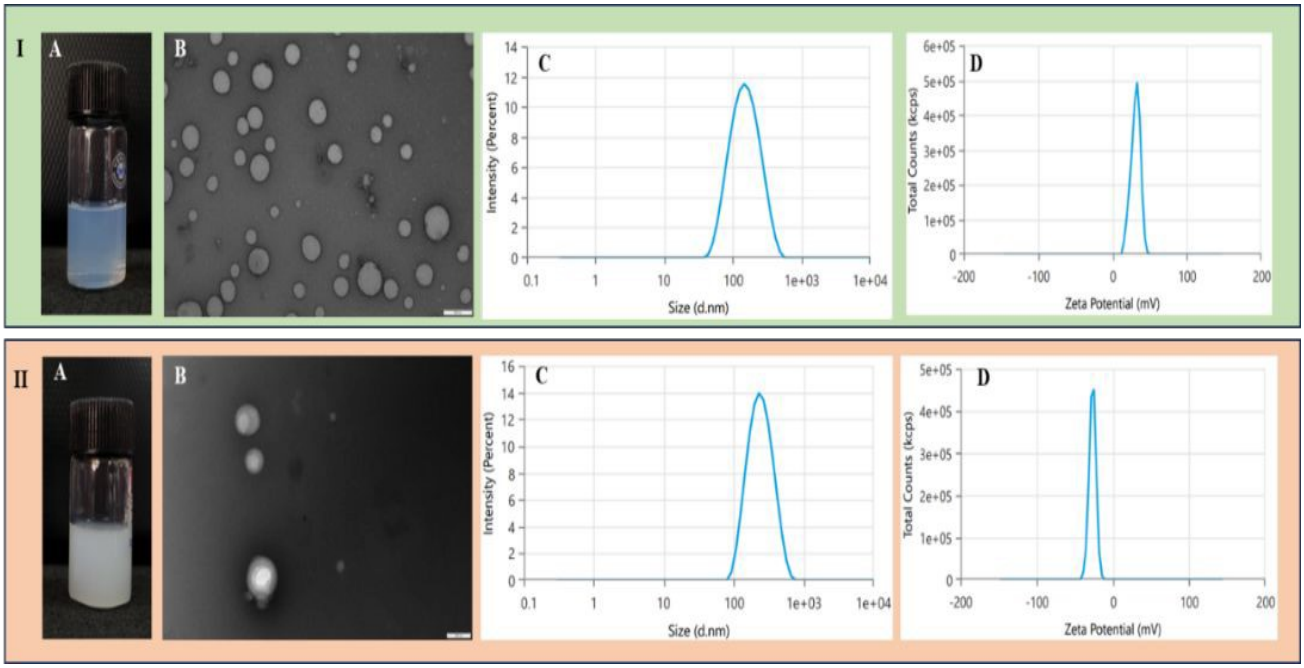

Figure 2: I) Lecithin chitosan nanoparticles, A) FZNP physical appearance with scale of 500 nm, B) TEM microscopic image of FZNP with scale of 200 nm, C) Particle size of FZNP, and D) Zeta potential of FZNP, II) Fucoidan coated lecithin chitosan nanoparticles, A) Fu-FZNP physical appearance, B) TEM microscopic image of Fu-FZNP, C) Particle size of Fu-FZNP, and D) Zeta potential of Fu-FZNP

3.2.2 Surface morphology of FZNP and Fu-FZNP

The surface morphology of the formulated FZNP and Fu-FZNP are illustrated in Figure 2IB and 2IIB. The nanoparticles were spherical with smooth surface and uniformly dispersed with no drug precipitation, which indicated the stability of the fabricated system.

View Article Online
DOI: 10.1039/D5PM00345H

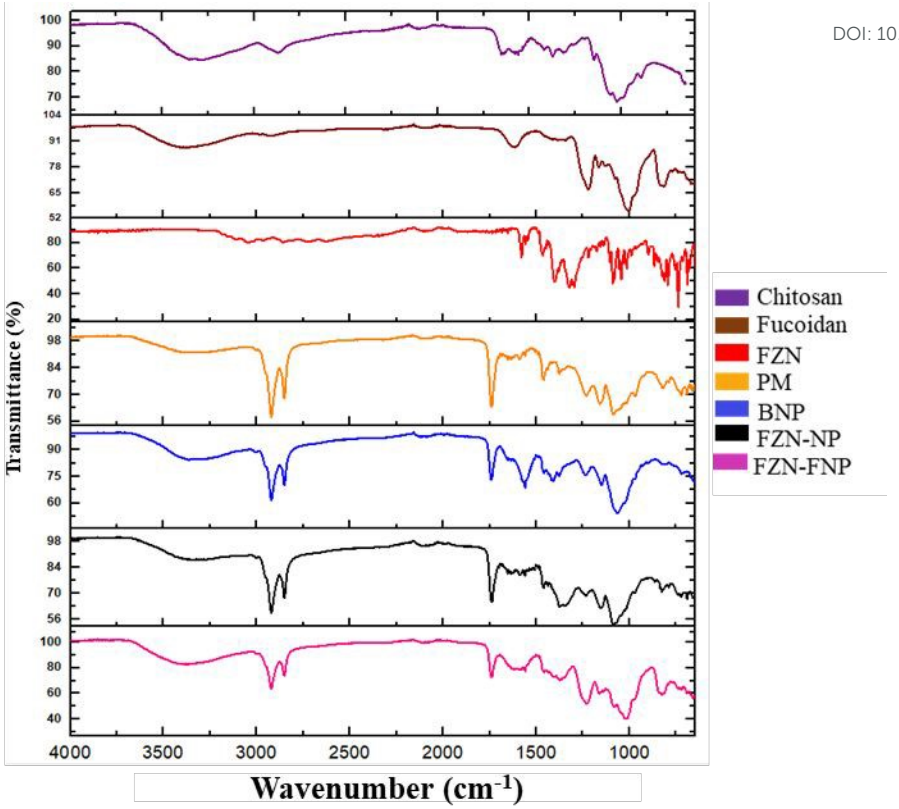

Figure 3: FTIR spectra of chitosan, fucoidan, FZN, PM, BNP, FZNP and Fu-FZNP.

3.2.3 ATR-FTIR Analysis of Nanoparticles

The ATR-FTIR analysis was carried out to investigate the compatibility of drug with excipients and drug encapsulation in the nanoparticles. The spectra of CH, Fu, Le, PM, BNP, FZNP, Fu-FZNP are compiled and displayed in Figure 3. The characteristic peaks corresponding to (C═N) of the imidazole group 1578 cm^{-1}, (C─H) 1465 cm^{-1}, ν(C=C) 1403 cm^{-1}, (C─N) 1295 cm^{-1}, (C─O─C) 1118 cm^{-1}, (C─S) 733 $cm^{-1}$and (C─Cl) 626 cm^{-1}were identified in FZN. The CH spectra exhibited C=N (1577 cm^{-1}); C=O (1653 cm^{-1}); C–O–C (1176 cm^{-1}); C–O (1054 cm^{-1}), Fu exhibited S=O (1165–1220 cm^{-1}); C–O–S (812 cm^{-1}) and C–H (2922 cm^{-1}, and 2853 cm^{-1}) stretching band of long fatty acid chain were observed for lecithin. The PM illustrated all the characteristic peaks pertaining to drug and excipients without formation of any new bonds indicating the absence of interaction between the drug and excipients. The FZNP and Fu-FZNP exhibited characteristic peaks of CH, Fu, Le with a red shift of peaks. The characteristic peaks of drug were not observed in FZNP and Fu-FZNP indicating the encapsulation of FZN in the nanoparticles.

View Article Online
DOI: 10.1039/D5PM00345H

3.2.4 DSC Analysis of Nanoparticles

Thermal events of CH, Fu, PM, BNP, FZNP, Fu-FZNP were observed using DSC and illustrated in Figure 4. The DSC thermogram of FZN exhibits an endothermic peak at 140°C, corresponding to the melting point of the crystalline FZN. On the other hand, the FZNP curve did not show the melting peak of the crystalline FZN, suggesting that the FZN has been uniformly dispersed in the polymer and lipid matrix. Similarly, FZN melting peak was absent in Fu-FZNP DSC curve, indicating that FZN dispersibility in FZNP persisted in the coated nanoparticles.

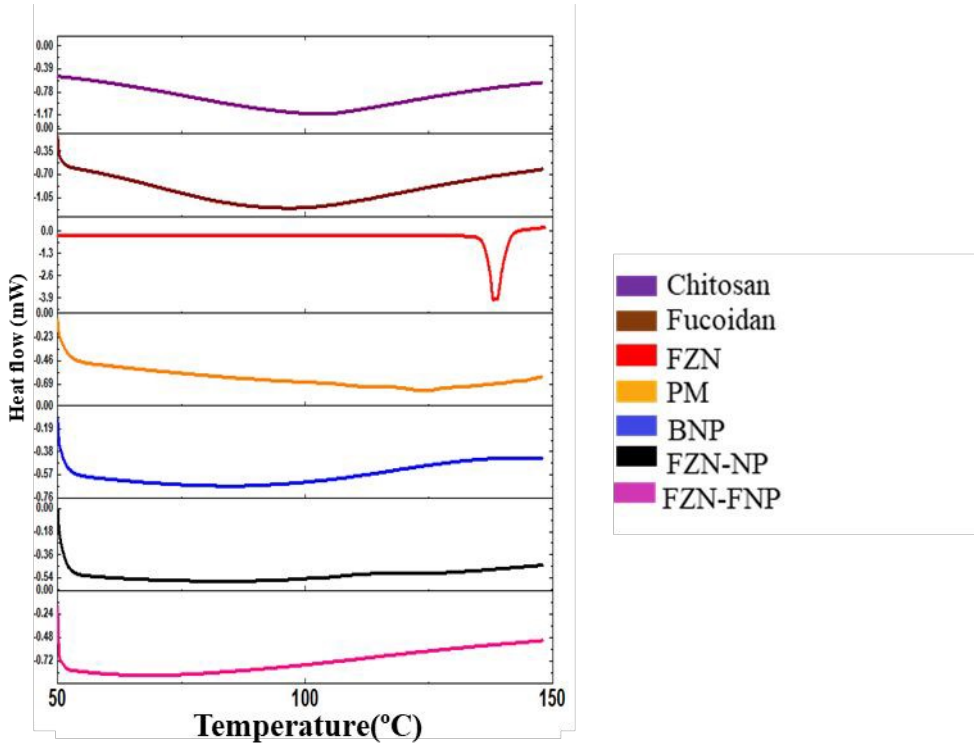

Figure 4: DSC thermograms of chitosan, fucoidan, FZN, PM, BNP, FZNP and Fu-FZNP.

3.2.5 P-XRD analysis of nanoparticles

The XRD of the samples was performed to estimate the form of FZN in FZNP and Fu-FZNP. The diffractograms of CH, Fu, PM, BNP, FZNP, Fu-FZNP are illustrated in Figure 5. The distinctive peaks of FZN were found absent in FZNP and Fu-FZNP. The peaks of the formulation and the polymer aligned, indicating the fact that the FZN was fully dispersed within the high concentrations of lipid-polymer and was enclosed in the nanoparticulate matrix. The diffractogram of the Fu-FZNP was in line with the Fu indicating the coating of the FZNP. These outcomes confirmed that FZN had been effectively encapsulated in FZNP and Fu-FZNP.

View Article Online
DOI: 10.1039/D5PM00345H

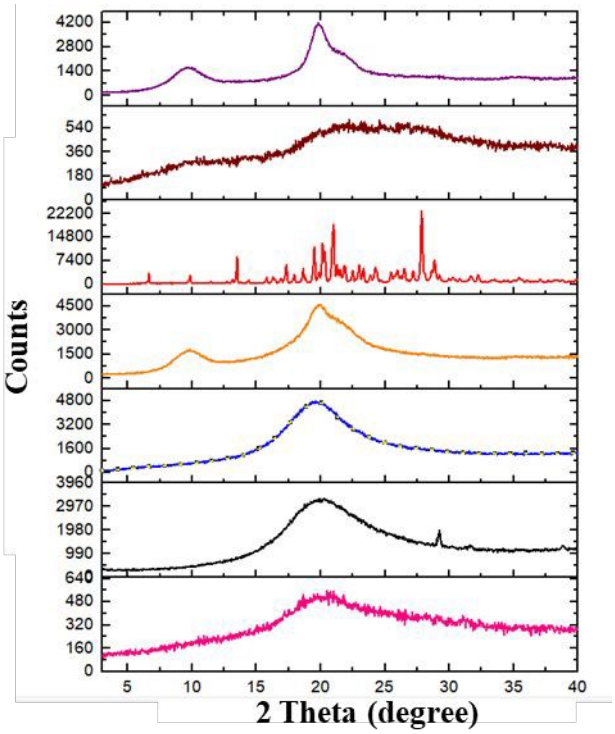

Figure 5: XRD data of chitosan, fucoidan, FZN, PM, BNP, FZNP and Fu-FZNP.

3.2.6 Entrapment efficiency

The FZNP and Fu-FZNP showed % EE of 65.47±2.32% and 71.13±5.74%. The % drug loading FZNP and Fu-FZNP is 11.69±0.41% and 7.41±0.60% respectively. The % entrapment efficiency of the fucoidan coated batch was approximately 7% more when compared to uncoated nanoparticles. The drug loading capacity of the uncoated nanoparticles was more when compared to coated nanoparticles as the modified particles included the weight of fucoidan coating polymer which in turn increased the net weight of nanoparticle.

3.2.7 *In-vitro* interaction of mucin with FZNP and Fu-FZNP

Mucus is a linear peptide chain consisting of 8-169 amino acids that has repeating proline, threonine, and serine domains. It is hydrophilic and highly negatively charged. The mucus prevents interactions between particles, it is highly effective at removing nanoparticles through a variety of adhesive interactions, including hydrogen bonding, hydrophobic, and electrostatic interaction potentials. The zeta potential and particle size of nanoparticles following co-incubation with mucin at 37°C are displayed in Figure 6IA and 6IB. It was observed that following a one-hour incubation period with mucus, the mean particle size of FZNP grew dramatically. This suggests that the particle was able to interface with the negatively charged mucin with ease and form a big complex because of strong electrostatic attraction. Nevertheless, the improvement of Fu-FZNP modification did not significantly increase the

View Article Online
DOI: 10.1039/D5PM00345H

particle sizes, suggesting the slightly interaction with the negatively charged mucin. Hence it can be assumed that the zeta potential altering nanoparticle i.e., Fu-FZNP didn't interact with negatively charged mucin.

3.2.8 *Ex-vivo* permeation studies

The impact of fucoidan coated lecithin chitosan nanoparticles on the permeability across the stratum corneum, skin permeation parameters were measured using FZNP and Fu-FZNP. The flux of the nanoparticles to transport the drug around the vaginal mucus of goat and the stratum corneum was shown by a graph showing the percentage cumulative amount of drug absorbed across the unit area of skin with respective time in Figure 6IC. The *ex-vivo* permeation studies through skin exhibited 61.74±2.07% and 72.11±1.4% of FZN from FZNP and Fu-FZNP, respectively as shown in Figure 6IC. The FZNP showed the flux of 151.21 μg/cm^2/h and followed by Fu-FZNP flux of 176.58 μg/cm^2/h. Figure 6II illustrates how intimate contact with superficial junctions may have allowed the superficial dispersion of active substances, leading to a possible modest penetration of rhodamine B solution. The findings concluded that Rhodamine B labeled FZN-NP and Fu-FZNP penetrate deep layers of excised goat vagina.

Figure 6: I) A) Particle size after interaction of Mucin with FZNP and Fu-FZNP, B) Zeta potential interaction of Mucin with FZNP and Fu-FZNP, and C) *Ex-vivo* permeation graph of FZNP and Fu-FZNP. The data is represented as mean±SD (n=3). II) Normal light microscopic images of goat vagina after application of A) Rhodamine B solution, B) Rhodamine B labeled FZN-NP C) Rhodamine B labeled Fu-FZNP after 12hr.Fluorescence images a) Rhodamine B solution, (b) Rhodamine B labeled FZN-NP c) Rhodamine B labeled Fu-FZNP after 12hr after 12hr.

3.2.9 Stability study of FZNP and Fu-FZNP

The stability studies data of FZNP and Fu-FZNP in illustrated in the Table 2. The stability parameter didn't show any significant change in the physical appearance, particle size, PDI, zeta potential and entrapment efficiency**.** Stability testing over longer durations (e.g., three months or more) in physiologically relevant media would provide a more comprehensive understanding of formulation performance and storage behavior. These aspects are planned to be addressed in future studies.

View Article Online
DOI: 10.1039/D5PM00345H

Table 2: Stability studies of FZNP and Fu-FZNP

Batch	Sample interval	Stability Conditions	Physical appearance	Particle size(nm)	PDI	Zeta potential	Entrapment efficicency (%)
FZNP	Initial	-	Bluish transparent	129.20±0.25	0.21±0.003	30.96±1.15	65.46±2.32
	1 month	5±3º C		130.20±0.62	0.20±0.004	32.74±1.70	62.01±1.63
		25±3º C		135.15±0.73	0.24±0.01	34.35±1.06	61.97±1.92
Fu-FZNP	Initial	-	Milky white	227.10±0.26	0.26±0.01	26.75±0.32	73.14±1.23
	1 month	5±3º C		228.83±0.85	0.27±0.008	29.89±0.38	70.09±2.39
		25±3º C		224.13±0.82	0.30±0.036	26.92±0.606	68.42±2.64

3.2.10 *In-vitro* antimicrobial activity

The results of qualitative antimicrobial activity of FZN, FZNP and Fu-FZNP by agar well diffusion method is reported in Figure 7I and 7II. The zone of inhibition values of FZNP and Fu-FZNP were 13.17±0.62 mm and 11.33±0.85 mm, respectively for *Staphylococcus aureus*. The zone of inhibition values of FZNP and Fu-FZNP were 19.83±0.94 mm and 21.67±0.47 mm, respectively for *Candida albicans*. The increase in concentration caused increases in the zone of inhibition.The developed formulations exibited both antibacterial and antifungal activity providing evidence to treat mixed infection in vagina. In the present study, antimicrobial activity was assessed using the agar well diffusion assay, which serves as a qualitative screening method to indicate inhibitory effects of the developed formulation. As the principal aim of this work was formulation optimization and preliminary biological evaluation, quantitative antimicrobial susceptibility tests such as minimum inhibitory concentration (MIC) determination and time–kill kinetics were not conducted. It is recognized that MIC and time–kill assays provide more precise and comprehensive measures of antimicrobial efficacy and kinetics than agar diffusion methods, and the lack of these assays represents a limitation of the current study. Future work will incorporate standardized MIC and time–kill analyses to

quantitatively evaluate the antimicrobial activity of the formulation and to substantiate its potential efficacy against mixed bacterial and fungal infections under defined conditions.

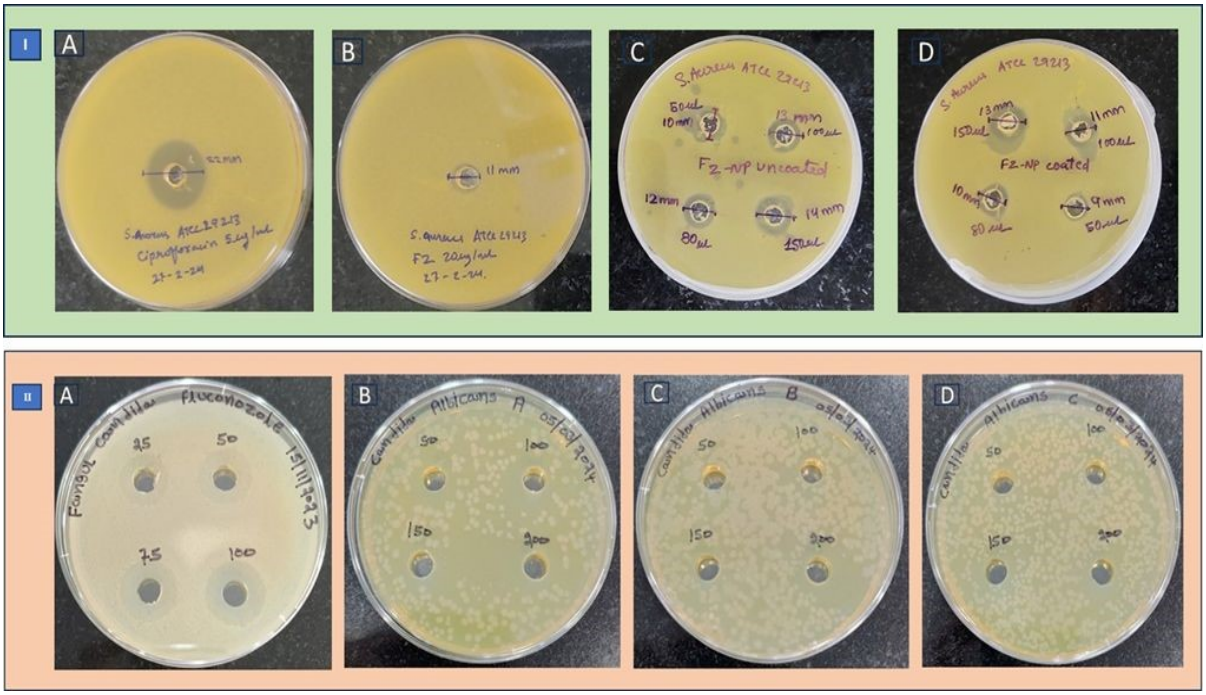

Figure 7: I) *In-vitro* antibacterial activity of patches against *Staphylococcus aureus,* A) Standard, B) FZN, C) FZNP, and D) Fu-FZNP II) *In-vitro* antifungal activity of patches against *Candida albicans,* A) Standard, B) FZN, C) FZNP, and D) Fu-FZNP

4. Conclusion

In the present investigation, lecithin chitosan nanoparticles and fucoidan coated nanoparticles loaded with FZN for the management of mixed vaginal infections were formulated and evaluated. The FZNP and Fu-FZNP were developed by ethanol injection technique, the nanoparticles displayed a mean particle size of 129.20±0.25 nm, PDI of 0.21±0.003 and zeta potential of +30.96±1.15 mV. Further the fucoidan coated zeta potential altering nanoparticles were prepared by incubating FZNP with Fucoidan. The optimized zeta potential altering nanoparticles displayed a mean particle size of 227.10±1.54 nm, PDI of 0.26±0.01 and zeta potential of -26.75±0.3 mV. The physicochemical characterization proved the encapsulation of the FZN in the nanoparticles and coating of fucoidan resulting in zeta potential altering nanoparticles to cross the mucus barrier prevent back diffusion. The entrapment efficiency of FZNP and Fu-FZNP were 65.47±2.32% and 71.13±5.74% with 11.69±0.414% (FZNP) and 7.41±0.60% (Fu-FZNP) drug loading. The morphology of the nanoparticles was spherically confirmed by microscopic images produced from TEM. The amount of drug permeated through excised goat vagina was found to be 61.74±2.07% and 72.11±1.4% for FZNP and Fu-FZNP.

View Article Online
DOI: 10.1039/D5PM00345H

The *in-vitro* antimicrobial activity of FZNP and Fu-FZNP showed antibacterial against *Staphylococcus aureus* and antifungal activity against *Candida albicans* species. These results indicated that FZN and Fu-FZNP lecithin chitosan nanoparticles might be further developed for safe, convenient, and effective treatment of mixed vaginal infections.

Conflict of Interest: The authors report no conflict of interest related to the manuscript.

FUNDING STATEMENT

The authors have no financial conflict with the subject matter or materials discussed in the manuscript.

CONFLICT OF INTEREST STATEMENT

The authors have no competing interests or relevant affiliations with any organization or entity with the subject matter or materials discussed in the manuscript.

View Article Online
DOI: 10.1039/D5PM00345H

5. References

[1] J. D. Sobel, C. Subramanian, B. Foxman, M. Fairfax, and S. E. Gygax, "Mixed vaginitis - More than coinfection and with therapeutic implications," *Curr Infect Dis Rep*, vol. 15, no. 2, pp. 104–108, Apr. 2013, doi: 10.1007/S11908-013-0325-5/METRICS.

[2] V. Goel, P. Bhalla, … A. S.-I. J. of S., and undefined 2011, "Lower genital tract infections in HIV-seropositive women in India," *journals.lww.comV Goel, P Bhalla, A Sharma, YM MalaIndian Journal of Sexually Transmitted Diseases and AIDS, 2011•journals.lww.com*, Accessed: Jun. 24, 2025. [Online]. Available: https://journals.lww.com/ijst/fulltext/2011/32020/lower_genital_tract_infections_in_hiv_seropositive.6.aspx

[3] J. Bornstein and D. Zarfati, "A Universal Combination Treatment for Vaginitis," *Gynecol Obstet Invest*, vol. 65, no. 3, pp. 195–200, Apr. 2008, doi: 10.1159/000111946.

[4] M. Sanguinetti, E. Cantón, R. Torelli, F. Tumietto, A. Espinel-Ingroff, and B. Posteraro, "In vitro activity of fenticonazole against Candida and bacterial vaginitis isolates determined by mono- Or dual-species testing assays," *Antimicrob Agents Chemother*, vol. 63, no. 7, 2019, doi: 10.1128/AAC.02693-18,.

[5] R. Albash, A. M. Al-Mahallawi, M. Hassan, and A. A. Alaa-Eldin, " Development and Optimization of Terpene-Enriched Vesicles (Terpesomes) for Effective Ocular Delivery of Fenticonazole Nitrate: In vitro Characterization and in vivo Assessment ," *Int J Nanomedicine*, vol. 16, pp. 609–621, Jan. 2021, doi: 10.2147/IJN.S274290.

[6] S. Veraldi and R. Milani, "Topical fenticonazole in dermatology and gynaecology: Current role in therapy," *Drugs*, vol. 68, no. 15, pp. 2183–2194, 2008, doi: 10.2165/00003495-200868150-00007.

[7] A. L. Costa, A. Valenti, and M. Veronese, "Study of the Morphofunctional Alterations Produced by Fenticonazole on Strains of Candida albicans, using the Scanning Electron Microscope (S. E. M.)," *Mycoses*, vol. 27, no. 1, pp. 29–35, Jan. 1984, doi: 10.1111/J.1439-0507.1984.TB01979.X.

[8] A. Costa, M. Veronese, P. Puggeri, and A. Valenti, "Ultrastructural findings of Candida albicans blastoconidia submitted to the action of fenticonazole.," *Arzneimittelforschung*, vol. 39, no. 2, pp. 230–233, Feb. 1989, Accessed: Jun. 24, 2025. [Online]. Available: https://europepmc.org/article/med/2659001

[9] J. Fernández-Alba *et al.*, "Fenticonazole Nitrate for Treatment of Vulvovaginitis: Efficacy, Safety, and Tolerability of 1-Gram Ovules, Administered as Ultra-Short 2-Day Regimen," *Journal of Chemotherapy*, vol. 16, no. 2, pp. 179–186, 2004, doi: 10.1179/JOC.2004.16.2.179.

[10] F. Gorlero, A. Sartani, C. Cordaro, … D. B.-… J. of C., and undefined 1988, "Fenticonazole tissue levels after the application of 3 different dosage forms of vaginal ovules.," *europepmc.orgF Gorlero, A Sartani, CI Cordaro, D Bertin, C Reschiotto, L De CeccoInternational Journal of Clinical Pharmacology, Therapy, and Toxicology, 1988•europepmc.org*, Accessed: Mar. 07, 2024. [Online]. Available: https://europepmc.org/article/med/3069750

[11] R. Albash, C. Yousry, A. M. Al-Mahallawi, and A. A. Alaa-Eldin, "Utilization of PEGylated cerosomes for effective topical delivery of fenticonazole nitrate: in-vitro characterization, statistical optimization, and in-vivo assessment," *Drug Deliv*, vol. 28, no. 1, pp. 1–9, 2021, doi: 10.1080/10717544.2020.1859000,.

[12] S. Veraldi and R. Milani, "Topical fenticonazole in dermatology and gynaecology: Current role in therapy," *Drugs*, vol. 68, no. 15, pp. 2183–2194, 2008, doi: 10.2165/00003495-200868150-00007,.

[13] S. Srikrishna and L. Cardozo, "The vagina as a route for drug delivery: A review," *Int Urogynecol J Pelvic Floor Dysfunct*, vol. 24, no. 4, pp. 537–543, Apr. 2013, doi: 10.1007/S00192-012-2009-3.

[14] C. M. Caramella, S. Rossi, F. Ferrari, M. C. Bonferoni, and G. Sandri, "Mucoadhesive and thermogelling systems for vaginal drug delivery," *Adv Drug Deliv Rev*, vol. 92, pp. 39–52, Sep. 2015, doi: 10.1016/j.addr.2015.02.001.

[15] R. Palmeira-de-Oliveira, A. Palmeira-de-Oliveira, and J. Martinez-de-Oliveira, "New strategies for local treatment of vaginal infections," *Adv Drug Deliv Rev*, vol. 92, pp. 105–122, Sep. 2015, doi: 10.1016/j.addr.2015.06.008.

[16] J. das Neves, R. Nunes, A. Machado, and B. Sarmento, "Polymer-based nanocarriers for vaginal drug delivery," *Adv Drug Deliv Rev*, vol. 92, pp. 53–70, Sep. 2015, doi: 10.1016/j.addr.2014.12.004.

[17] G. Chindamo, S. Sapino, E. Peira, D. Chirio, and M. Gallarate, "Recent advances in nanosystems and strategies for vaginal delivery of antimicrobials," *Nanomaterials*, vol. 11, no. 2, pp. 1–29, Feb. 2021, doi: 10.3390/NANO11020311,.

[18] B. Valamla *et al.*, "Engineering drug delivery systems to overcome the vaginal mucosal barrier: Current understanding and research agenda of mucoadhesive formulations of

vaginal delivery," *J Drug Deliv Sci Technol*, vol. 70, Apr. 2022, doi: 10.1016/J.JDDST.2022.103162.

[19] J. das Neves, M. Amiji, and B. Sarmento, "Mucoadhesive nanosystems for vaginal microbicide development: Friend or foe?," *Wiley Interdiscip Rev Nanomed Nanobiotechnol*, vol. 3, no. 4, pp. 389–399, Jul. 2011, doi: 10.1002/WNAN.144,.

[20] R. Bansil and B. S. Turner, "Mucin structure, aggregation, physiological functions and biomedical applications," *Curr Opin Colloid Interface Sci*, vol. 11, no. 2–3, pp. 164–170, Jun. 2006, doi: 10.1016/J.COCIS.2005.11.001.

[21] K. Netsomboon and A. Bernkop-Schnürch, "Mucoadhesive vs. mucopenetrating particulate drug delivery," *European Journal of Pharmaceutics and Biopharmaceutics*, vol. 98, pp. 76–89, Jan. 2016, doi: 10.1016/J.EJPB.2015.11.003.

[22] B. Le-Vinh, N. M. N. Le, I. Nazir, B. Matuszczak, and A. Bernkop-Schnürch, "Chitosan based micelle with zeta potential changing property for effective mucosal drug delivery," *Int J Biol Macromol*, vol. 133, pp. 647–655, Jul. 2019, doi: 10.1016/J.IJBIOMAC.2019.04.081.

[23] L. M. Hemmingsen, N. Škalko-Basnet, and M. W. Jøraholmen, "The expanded role of chitosan in localized antimicrobial therapy," *Mar Drugs*, vol. 19, no. 12, Dec. 2021, doi: 10.3390/MD19120697,.

[24] K. A. Janes, P. Calvo, and M. J. Alonso, "Polysaccharide colloidal particles as delivery systems for macromolecules," *Adv Drug Deliv Rev*, vol. 47, no. 1, pp. 83–97, Mar. 2001, doi: 10.1016/S0169-409X(00)00123-X.

[25] S. A. Agnihotri, N. N. Mallikarjuna, and T. M. Aminabhavi, "Recent advances on chitosan-based micro- and nanoparticles in drug delivery," *Journal of Controlled Release*, vol. 100, no. 1, pp. 5–28, Nov. 2004, doi: 10.1016/J.JCONREL.2004.08.010.

[26] "Stabilization of colloidal systems by the formation of ionic lipid-polysaccharide complexes," May 1996.

[27] S. Batzri and E. D. Korn, "Single bilayer liposomes prepared without sonication," *Biochimica et Biophysica Acta (BBA) - Biomembranes*, vol. 298, no. 4, pp. 1015–1019, Apr. 1973, doi: 10.1016/0005-2736(73)90408-2.

[28] "Liposome Drug Delivery Systems - Guru V. Betageri, Scott Allen Jenkins, Daniel Parsons - Google Books." Accessed: Jun. 27, 2025. [Online]. Available: https://books.google.co.in/books?hl=en&lr=&id=RI8sEQAAQBAJ&oi=fnd&pg=PP1&dq=G.+V.+Betageri,+S.+A.+Jenkins,+and+D.+L.+Parsons,+Liposome+drug+delivery+systems.+Technomic+Pub,+1993.+Accessed:+Mar.+07,+2024.+%5BOnline%5D.+

Available:+https://www.routledge.com/Liposome-Drug-Delivery-Systems/Betageri-Jenkins-Parsons/p/book/9781566760300&ots=0pe8hiVm4f&sig=XJJljDOyh35YwuaoqGbRGIbumNE&redir_esc=y#v=onepage&q&f=false

[29] H. Takeuchi, Y. Matsui, H. Yamamoto, and Y. Kawashima, "Mucoadhesive properties of carbopol or chitosan-coated liposomes and their effectiveness in the oral administration of calcitonin to rats," *Journal of Controlled Release*, vol. 86, no. 2–3, pp. 235–242, Jan. 2003, doi: 10.1016/S0168-3659(02)00411-X.

[30] I. Henriksen, S. R. Vågen, S. A. Sande, G. Smistad, and J. Karlsen, "Interactions between liposomes and chitosan II: Effect of selected parameters on aggregation and leakage," *Int J Pharm*, vol. 146, no. 2, pp. 193–203, Jan. 1997, doi: 10.1016/S0378-5173(96)04801-6.

[31] I. Henriksen, G. Smistad, and J. Karlsen, "Interactions between liposomes and chitosan," *Int J Pharm*, vol. 101, no. 3, pp. 227–236, Jan. 1994, doi: 10.1016/0378-5173(94)90218-6.

[32] E. A. Ho, V. Vassileva, C. Allen, and M. Piquette-Miller, "In vitro and in vivo characterization of a novel biocompatible polymer–lipid implant system for the sustained delivery of paclitaxel," *Journal of Controlled Release*, vol. 104, no. 1, pp. 181–191, May 2005, doi: 10.1016/J.JCONREL.2005.02.008.

[33] J. Grant, M. Blicker, M. Piquette-Miller, and C. Allen, "Hybrid films from blends of chitosan and egg phosphatidylcholine for localized delivery of paclitaxel," *J Pharm Sci*, vol. 94, no. 7, pp. 1512–1527, Jul. 2005, doi: 10.1002/JPS.20379.

[34] F. Sonvico *et al.*, "Formation of self-organized nanoparticles by lecithin/chitosan ionic interaction," *Int J Pharm*, vol. 324, no. 1, pp. 67–73, Oct. 2006, doi: 10.1016/J.IJPHARM.2006.06.036.

[35] I. A. Walbi *et al.*, "Development of a Curcumin-Loaded Lecithin/Chitosan Nanoparticle Utilizing a Box-Behnken Design of Experiment: Formulation Design and Influence of Process Parameters," *Polymers (Basel)*, vol. 14, no. 18, Sep. 2022, doi: 10.3390/POLYM14183758,.

[36] L. M. Hemmingsen, V. Panzacchi, L. M. Kangu, B. Giordani, B. Luppi, and N. Škalko-Basnet, "Lecithin and Chitosan as Building Blocks in Anti-Candida Clotrimazole Nanoparticles," *Pharmaceuticals*, vol. 16, no. 6, Jun. 2023, doi: 10.3390/PH16060790,.

[37] A. Hafner, J. Lovrić, D. Voinovich, and J. Filipović-Grčić, "Melatonin-loaded lecithin/chitosan nanoparticles: Physicochemical characterisation and permeability

through Caco-2 cell monolayers," *Int J Pharm*, vol. 381, no. 2, pp. 205–213, Nov. 2009, doi: 10.1016/J.IJPHARM.2009.07.001.

[38] T. Q, L. W, G. C, and Z. G, "Preparation and evaluation of quercetin-loaded lecithin-chitosan nanoparticles for topical delivery," *Int J Nanomedicine*, vol. 6, p. 1621, Aug. 2011, doi: 10.2147/IJN.S22411.

[39] I. Özcan, E. Azizoğlu, T. Senyiğit, M. Özyazici, and Ö. Özer, "Enhanced dermal delivery of diflucortolone valerate using lecithin/chitosan nanoparticles: in-vitro and in-vivo evaluations," *Int J Nanomedicine*, vol. 8, pp. 461–475, Jan. 2013, doi: 10.2147/IJN.S40519.

[40] M. Saha *et al.*, "QbD based development of resveratrol-loaded mucoadhesive lecithin/chitosan nanoparticles for prolonged ocular drug delivery," *J Drug Deliv Sci Technol*, vol. 63, Jun. 2021, doi: 10.1016/J.JDDST.2021.102480.

[41] A. Sosnik, J. Das Neves, and B. Sarmento, "Mucoadhesive polymers in the design of nano-drug delivery systems for administration by non-parenteral routes: A review," *Prog Polym Sci*, vol. 39, no. 12, pp. 2030–2075, 2014, doi: 10.1016/J.PROGPOLYMSCI.2014.07.010.

[42] K. Netsomboon and A. Bernkop-Schnürch, "Mucoadhesive vs. mucopenetrating particulate drug delivery," *European Journal of Pharmaceutics and Biopharmaceutics*, vol. 98, pp. 76–89, Jan. 2016, doi: 10.1016/J.EJPB.2015.11.003.

[43] T. M. M. Ways *et al.*, "Mucus-penetrating nanoparticles based on chitosan grafted with various non-ionic polymers: Synthesis, structural characterisation and diffusion studies," *J Colloid Interface Sci*, vol. 626, pp. 251–264, Nov. 2022, doi: 10.1016/J.JCIS.2022.06.126,.

[44] N. Rajana *et al.*, "Targeted delivery and apoptosis induction of CDK-4/6 inhibitor loaded folic acid decorated lipid-polymer hybrid nanoparticles in breast cancer cells," *Int J Pharm*, vol. 651, p. 123787, Feb. 2024, doi: 10.1016/J.IJPHARM.2024.123787.

[45] N. Rajana *et al.*, "Fabrication and characterization of teriflunomide-loaded chondroitin sulfate hybridized zein nanoparticles for the management of triple negative breast cancer," *Int J Biol Macromol*, vol. 300, p. 140316, Apr. 2025, doi: 10.1016/J.IJBIOMAC.2025.140316.

[46] Y. S. Pooja, N. Rajana, R. Yadav, L. T. Naraharisetti, C. Godugu, and N. K. Mehra, "Design, development, and evaluation of CDK-4/6 inhibitor loaded 4-carboxy phenyl boronic acid conjugated pH-sensitive chitosan lecithin nanoparticles in the management

of breast cancer," *Int J Biol Macromol*, vol. 258, p. 128821, Feb. 2024, doi: 10.1016/J.IJBIOMAC.2023.128821.

[47] P. S. Chary *et al.*, "Enhancing breast cancer treatment: Comprehensive study of gefitinib-loaded poloxamer 407/TPGS mixed micelles through design, development, in-silico modelling, In-Vitro testing, and Ex-Vivo characterization," *Int J Pharm*, vol. 657, p. 124109, May 2024, doi: 10.1016/J.IJPHARM.2024.124109.

[48] S. Shaikh, P. S. Chary, O. Khan, and N. K. Mehra, "Development and evaluation of nilotinib-loaded Bovine Serum Albumin nanoparticles: In-vitro and in-silico insights," *Int J Biol Macromol*, vol. 308, p. 142185, May 2025, doi: 10.1016/J.IJBIOMAC.2025.142185.

[49] A. Mammella, V. Bhavana, P. S. Chary, U. Anuradha, and N. K. Mehra, "Modulation of chondroprotective hyaluronic acid and poloxamer gel with Ketoprofen loaded transethosomes: Quality by design-based optimization, characterization, and preclinical investigations in osteoarthritis," *Int J Biol Macromol*, vol. 280, p. 135919, Nov. 2024, doi: 10.1016/J.IJBIOMAC.2024.135919.

[50] N. U. Kumari, P. S. Chary, E. Pardhi, and N. K. Mehra, "Tailoring micellar nanocarriers for pemetrexed in breast cancer: design, fabrication and in vitro evaluation," *Nanomedicine*, May 2024, doi: 10.2217/NNM-2024-0013.

[51] P. S. Chary *et al.*, "Enhancing breast cancer treatment: Comprehensive study of gefitinib-loaded poloxamer 407/TPGS mixed micelles through design, development, in-silico modelling, In-Vitro testing, and Ex-Vivo characterization," *Int J Pharm*, vol. 657, p. 124109, May 2024, doi: 10.1016/J.IJPHARM.2024.124109.

[52] W. Zhou *et al.*, "Mucus-penetrating dendritic mesoporous silica nanoparticle loading drug nanocrystal clusters to enhance permeation and intestinal absorption," *Biomater Sci*, vol. 11, no. 3, pp. 1013–1030, Dec. 2023, doi: 10.1039/D2BM01404A.

[53] R. Albash, M. A. El-Nabarawi, H. Refai, and A. A. Abdelbary, "Tailoring of PEGylated bilosomes for promoting the transdermal delivery of olmesartan medoxomil: in-vitro characterization, ex-vivo permeation and in-vivo assessment," *Int J Nanomedicine*, vol. 14, pp. 6555–6574, 2019, doi: 10.2147/IJN.S213613.

View Article Online
DOI: 10.1039/D5PM00345H

Data Availability: Data will be available upon request